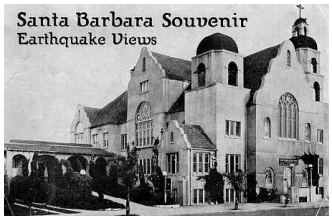

4th IASPEI / IAEE International Symposium:

Effects of Surface Geology on Seismic Motion

August 23–26, 2011 · University of California Santa Barbara

A Preliminary Result of Shallow S-wave Velocity Structures in the Taipei Basin

Chun-Hsiang Kuo, Tao-Ming Chang, Che-Min Lin
National Center for Research on Earthquake Engineering
Taipei, Taiwan
ROC

Kuo-Liang Wen
National Central University
Taoyuan, Taiwan
ROC

ABSTRACT

Many researches of strong motion simulations in the Taipei Basin were carried out due to its significant site effects and the important statuses of administration and economics in Taiwan. However, no reliable S-wave velocity structure of the sedimentary layers as well as the covered Tertiary bedrocks in the Taipei Basin was obtained. The near-surface S-wave velocity structure is very important for the characteristics of strong ground motion, so we conducted array measurements of microtremor inside the Taipei Basin and used the PS-logging profiles of the Engineering Geological Database of TSMIP (EGDT) and the Taipei downhole arrays to construct the S-wave velocity structure, which contains the basement and the very shallow part (within top 30 meters), might be particularly important for strong ground motion estimations. We therefore developed a joint inversion technique of phase velocities and HVSRs to increase the probing depth of the microtremor arrays, which were deployed in elementary schools for convenience and thus the array sizes were constricted. The extrapolation named BCV (Bottom Constant Velocity) was adopted to estimate the Vs30 for dozens of PS-logging profiles of EGDT which do not reach 30 meters. Consequently, the preliminary S-wave velocity structure of the Taipei Basin includes the basement and the very shallow part was therefore initially completed.

INTRODUCTION

It has been recognized that soft and young sediments covering on firm bedrock can amplify seismic waves and cause severe damage during an enormous earthquake. Therefore, it is very important to understand S-wave velocity structure of soft sediments. Otherwise, averaged S-wave velocity of the top 30 m strata (Vs30) is considered a substantial influence on the characteristics of ground motions. The National Earthquake Hazards Reduction Program (NEHRP) recommended Vs30 as a significant indicator for classifying sites in the recent building code (BSSC, 2001). According to the research of Anderson et al. (1996), the influence of top 30 m sediments is indicated great for ground motion characteristics even though the thickness is almost never reach 1% of the depth to a hypocenter.

There are many techniques proposed in the past decades to evaluate shallow S-wave velocity profiles. Seismic refraction, reflection, ReMi (Refraction Micotremor) (Louie, 2001; Pancha et al., 2008), SASW (Spectra Analysis of Surface Wave), and MASW (Multichannel Analysis of Surface Waves) are all well-known noninvasive techniques for estimating S-wave velocities. Some methods are sensitive in shallow layers due to the high-frequency source, for example, Williams et al. (2007) conducted the high-resolution seismic refraction and reflection methods to derive the S-wave velocity profiles and Vs30 in the St. Louis, USA. In contrast, down-hole, up-hole, cross-hole and suspension PS-logging are popular invasive techniques. The invasive methods are considered the comparative accurate technique to measure the velocity profiles. For example, Bang and Kim (2007) adopted the SPT-uphole method to determine S-wave velocity profiles for comparison with profiles determined by down-hole and SASW methods. Furthermore, passive source techniques such as microtremor array method are also becoming popular in recent studies (Arai and Tokimatsu, 2008; Fäh et al., 2008; García-Jerez et al., 2007; Kuo et al., 2009). Kuo et al. (2009) estimated S-wave velocity profiles by SWPM (the combo of SASW and IR method), microtremor array, and PS-logging in shallow subsurface layers, and then considered the suspension PS-logging method as being able to observe precise P and S-wave velocities in the one-dimensional borehole measurement. Boore and Asten (2008) compared S-wave slowness profiles obtained by various invasive (suspension PS-logging, surface source-downhole receiver, and cross-hole) and noninvasive (HVSR of single station, high resolution reflection/refraction, SASW, MASW, and microtremor array) methods at several sites in the Santa Clara Valley, California.

Over the past two decades, many researches of estimating S-wave velocities by using microtremor arrays were published. Microtremor array method has a significant advantage than the traditional reflection/refraction methods, that is, easy to conduct even in a populous downtown. Micotremor array method does not need drilling or explosive source that usually can not be accepted by community because of the annoying noise. This advantage has made microtremor method become a more popular technique because of the global urbanization. Furthermore, the microtremor is caused be sea tide, wind, human activities, etc., it takes shorter time and lower cost to gather a satisfactory number of data then waiting for enough earthquakes. Those describes above are the reasons that related studies of microtremor are getting much more than before in recent years. In the late 1950s, Aki (1957) proposed the analysis of seismic noise as a good tool for investigating S-wave velocity structures. He utilized small-scale circular seismic arrays to derive the phase-velocity dispersion curve by correlating noise records. The method he proposed to derive phase velocities is called SPatial AutoCorrelation (SPAC) method. Capon (1969) proposed the maximum likelihood (also called high-resolution method) of frequency-wavenumber (F-K) method to determine the vector velocities of propagating seismic waves using Large Aperture Seismic Arrays (LASA), a method that provides seismic data to facilitating the discernment between earthquake and underground nuclear explosions. Hereafter, a Rayleigh wave inversion technique using array records of microtremor was proposed as a useful exploration method for obtaining the S-wave velocity structures of sedimentary layers. The SPAC and F-K techniques are both primary approaches to obtain phase velocities of Rayleigh waves of fundamental mode. Array exploration of microtremor was established by Horike (1985) and Matsushima and Okada (1990) after the pioneering work done by Aki (1957). They used long-period microtremors to estimate deep S-wave velocity structures. After that, Sato et al. (1991) and Malagnini et al. (1993) used short-period microtremor to estimate S-wave velocity profiles of shallow layers. Recently, Kawase et al. (1998) and Satoh et al. (2001a, 2001b) succeeded in estimating shallow and deep S-wave velocity structures at several sites in America, Sendai Basin, and Taichung Basin using both short and long-period microtremor. This method is based on the assumption that microtremor is dominated by surface waves (Rayleigh and Love waves) and the structures of measured sites are not sharply varying in the horizontal. Except for estimating S-wave velocity profiles, microtremor is also used to assess site responses, i.e., resonant frequency and amplification factor, since Nakamura (1989) proposed a Horizontal to Vertical Spectra Ratio (HVSR) method for earthquake and microtremor. He considered that a seismic noise tends to induce Rayleigh waves in vertical component because the surface artificial sources have mostly prevailing vertical motions. Therefore, Rayleigh waves are assumed as noise of microtremor and the HVSR method to eliminate the influence of Rayleigh waves was proposed. Another important contribution of the article was proposed a single-station spectral ratio method so that scientists do not have to find a reference site when they investigated site response. Many researches adopted the convenient single-station HVSR method to investigate site response using earthquake (Lermo and Chavez-Garcia, 1993; Chaves-Garcia et al., 1996; Bonilla et al., 1997; Tsuboi et al., 2001; Wen et al., 2006) or microtremor recordings (Bodin and Horton, 1999; Bodin et al., 2001; Woolery and Street, 2002) thereafter. Since 2000, numbers of literatures about microtremor are growing explosively. At first, scientists compared the S-wave velocities estimated by microtremor arrays with those derived by other traditional geophysical techniques, such as seismic refraction, reflection, downhole, etc. However, some existing geophysical profiles were at a distance from the measured site of microtremor (Parolai et al., 2005). By contrast, some others compared with nearby and various geotechnical methods (Louie, 2001; Arai and Tokimatsu, 2004, 2005; Boore and Asten, 2008; Kuo et al., 2009). Meanwhile, the inversions of HVSR of microtremor were proposed (Fäh et al., 2001, 2003; Arai and Tokimatsu, 2004) and to be used together with dispersion curves to make the estimated S-wave velocity profiles more accurate, especially for the depth of engineering bedrock. Nakamura (2007) identified his assumption that "*the peak of the H/V is mostly caused by the multiple-reflection of SH waves and etc.*" He also found that dispersion curves of microtremor array measurements are sometimes unstable near the dominate frequency of HVSR and he believed this was because the prominent peak of HVSR is mostly caused by the multiple reflection of SH waves, rather than Rayleigh waves. The proposed joint inversion in the study was based on Nakamura's assumption that although microtremor contains abundant Rayleigh waves, after the procedure of HVSR, SH-waves are the major constituent near the dominant frequency because the Rayleigh waves were eliminated.

The EGDT is constructed by the National Center for Research on Earthquake Engineering (NCREE) and Central Weather Bureau (CWB) from 2000. Kuo et al. (2011a) proposed an accurate extrapolation, that is, BCV to estimate the Vs30 for those S-wave velocity profiles less than 30 m in the EGDT. A strong motion downhole array and a broadband seismic array in the Taipei Basin were deployed by the Institute of Earth Science, Academia Sinica. The velocity profiles at six of the stations of the two arrays were measured by a suspension PS-logger system before the seismometers were installed. The logged S-wave velocity profiles were used to sketch the distribution of Vs30 in the Taipei Basin in this study.

DATA ACQUISTION

The S-wave velocity profiles utilized in this study were derived from microtremor arrays and PS-logging measurements. The microtremor array measurements were conducted at 12 TSMIP sites, at which the space was barely enough for the array deployments in such a crowed city; moreover, the logged velocity profiles were good comparable objects in the shallow part for the development of the joint inversion technique. The logging data we used to delineate the distribution of Vs30 in the Taipei Basin included 68 free-field TSMIP stations of the EGDT in the Taipei region and six stations of the Taipei downhole arrays in the basin.

Measurements of Microtremor Array

The measurements of microtremor array were implemented using portable instruments – Tokyo Sokushin portable servo seismometers. A set of the instrument contains a recorder SAMTAC-801B and a sensor VSE311C or VSE315D. SAMTAC-801B is a 24-bit recorder with a MO access device. VSE311C or VSE315D is a six-channel (three velocities and three accelerations) seismometer with flat amplitude from 0.1 to 50 Hz. The internal clock was corrected by a global positioning system (GPS) before each measurement to ensure the observations of all instruments were simultaneous. Ten instruments were used for a microtremor array measurement and they were arranged on the center and the vertexes of three concentric equilateral triangles in each measurement as in Fig. 1. We tried to spread the instruments such as shown at the right of Fig. 1, but the configuration of larger arrays usually tended to be distorted as in the left due to obstacles such as buildings. Depending on the space of each site, we conducted one or two arrays and the radii were also variable from site to site. The sampling rate was 100 points per second in all of our microtremor array measurements. Fig. 2 illustrated recordings of an array observation. The recordings showed similar waveforms at the same time sections and good correlations between different recordings.

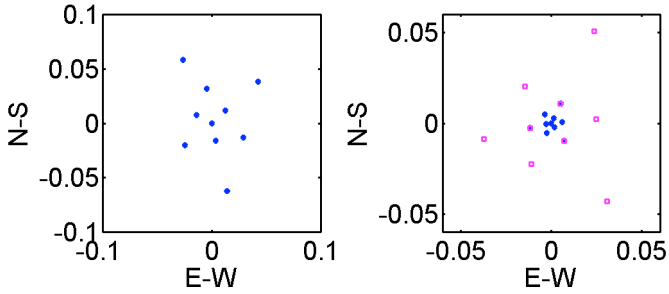

Fig. 1. The array configurations spread at TAP022 (left) and TAP007 (right). The open pink squares were the large array; the solid diamonds were the small. Both arrays had the same center. Only one array was deployed at TAP022 and two array measurements were conducted at TAP007. The unit of length in NS and EW directions is kilometer. The maximum radii were 64 m at TAP022 and 56 m at TAP007.

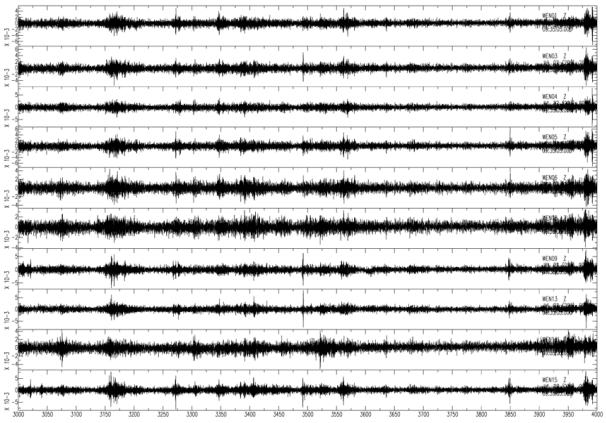

Fig. 2. Time history of the vertical component of an array recording. Similar waveforms were recorded at the same time segments by different instruments.

Vs30 from logging data

In Taiwan, the NCREE and CWB have been launching a multi-year drilling project on free-field TSMIP stations to construct the EGDT since 2000. We used the Vs30 values calculated and estimated by Kuo et al. (2011b) at 68 free-field TSMIP stations in the Taipei region; otherwise, we also requested the logged profiles at six stations of the Taipei downhole arrays together to delineate the distribution of Vs30 in the Taipei Basin. The S-wave velocity profiles at ten stations of the EGDT in the Taipei region were less than 30 m and thus the Vs30 were extrapolated by the BCV method (Kuo et al., 2011b).

METHODOLOGY OF MICROTREMOR ARRAY ANALYSIS

The techniques used to analyze the recordings of the microtremor arrays and estimate the S-wave velocity profiles were introduced in the following sections.

Frequency-Wavenumber (F-K)

In the microtremor array analysis, natural surface vibrations were observed by ten sensors, which were roughly arranged on a triple-triangle array. The high-resolution F-K method (Capon, 1969) is a widely-used technique in deriving the phase velocities. This method allowed the arrangement of instruments to be an arbitrary shape during the field works. F-K method assumes that random horizontal plane waves are propagating through sensors of an array on the surface. Using a given frequency, k_x, and k_y (wavenumbers in x and y directions) to calculate the relative arrival time of each sensor, and then the phases were shifted according to the delayed time. Consequently, a power spectrum was derived from the stacked waves. The location of the maximum value of a power spectrum in the (k_x, k_y) plane gives the phase velocity and the azimuth of the propagating wave on a certain frequency through the array. It should be noted that the high-resolution F-K method (Capon, 1969; Aki and Richards, 1980) is an improved F-K approach, which adopted the maximum likelihood estimation to increase the resolution, and thus the high-resolution method is more capable of distinguishing two waves traveling on close wavenumbers than the conventional one. High-resolution F–K analysis was utilized to identify the phase velocities using only the vertical velocity recordings of the microtremor arrays in this study. The vertical velocity component derived from the observed recordings was used with different window lengths of 512, 1024, 2048, 4096, and 8192 points by moving the window 200 points in each step. After this procedure, a cross-correlation of each recording of the same array was performed to increase the signal to noise ratio and then conducted a 2D Fourier transform based on the maximum likelihood method to obtain the F–K spectra.

The high-resolution F–K spectral analysis method assumed that the data $d_{i,t}$ in station i is composed of signal $S_{i,t}$ and noise $n_{i,t}$, then we can write data d_i as $d_{i,t} = S_{i,t}+n_{i,t}$, where $i = 1, \ldots, N$, and t is the discrete time. If time is the same, $d_i = S_i+n_i$, where $i = 1, \ldots, N$. Assume d_i conforms to a Gaussian distribution, and its mean value is S, then the covariance matrix can be written as $R_{i,j} = \langle n_i n_j \rangle$, and

$$F(d_i .....d_N) = \frac{|\phi|^{1/2}}{(2\pi)^{N/2}} \exp\left[-\frac{\pi}{2}\sum_{i,j=1}^{N}\phi_{ij}(d_i - S)(d_j - S)\right] \quad (1)$$

Equation (1) is called the Joint Probability Density Function, where ϕ_{ij} is the inverse matrix of $R_{i,j}$, and ϕ is the value of ϕ_{ij}. In order to obtain a better signal, i.e., maximize Equation (1), we must choose S to minimize the value of

$$\sum_{i,j=1}^{N}\phi_{ij}(d_i - S)(d_j - S) \quad (2)$$

Taking the derivative of Equation (2) respect to S and setting it equal to zero. We can find that the minimum occurs when

$$S = \sum_{i,j=1}^{N}\phi_{ij}d_i \Big/ \sum_{i,j=1}^{N}\phi_{ij} \quad (3)$$

Equation (3) is the weighting of each sensor and is directly proportional to the sum of ϕ_{ij}. Capon (1969) performed the maximum likelihood method to obtain the F-K power spectra by utilizing the previous approach and got

$$P(k_x, k_y, \omega) = \{\sum_{i=1}^{N}\sum_{j=1}^{N}\phi_{ij}(\omega)\exp[ik_x(x_i - x_j) + ik_y(y_i - y_j)]\}^{-1} \quad (4)$$

, where $\phi_{ij}(\omega)$ is an element of $\phi(\omega)$, and x_i and y_i is the coordinate of i^{th} sensor. Capon used this method in separating various modes of waves traveling across the LASA. In addition, the application of high-resolution F-K method is also used to other research areas, such as radar, astronomy, and sonar.

Transfer Function of SH waves

As mentioned previously, the resonant peak on the dominate frequency of HVSR of microtremor is mainly composed of multi-reflected SH waves according to Nakamura's theory, rather than fundamental or higher mode Rayleigh waves. The transfer function of SH waves, which was accomplished by Haskell (1960), was adopted to simulate the HVSR of microtremor in this study. The plane layer response of SH waves were proposed by Haskell (1953, 1960), which is a simple case because there is no coupling wave types. According to Snell's law,

$$c = \frac{\beta_1}{\sin j_1} = \frac{\beta_2}{\sin j_2} = \frac{\beta_3}{\sin j_3} \ldots = \frac{\beta_n}{\sin j_n} \tag{5}$$

, where c is the phase velocity related to the incidence angle j_n of the n^{th} layer, and β_n is the Vs of the n^{th} layer. Following Haskell's result (Haskell 1953, Equation 9.8) and setting the transverse shear stress equal to zero at the free surface, then we obtained

$$\begin{aligned} S_n^{\searrow} + S_n^{\nearrow} &= A_{11} S_0 \\ S_n^{\searrow} - S_n^{\nearrow} &= A_{21} S_0 / \mu_n r_{\beta n} \end{aligned} \tag{6}$$

, where S_n means the amplitude of SH waves, as for the upward and downward arrows of superscript indicate the directions of traveling SH waves and the subscript n denote the n^{th} layer. Moreover, $r_{\beta n} = [(c/\beta)^2 - 1]^{1/2}$; μ_n is shear modulus; A_{kl} is one element of the 2×2 matrix a_n, which was defined for the layer by

$$a_n = \begin{pmatrix} \cos Q_n & i\mu_n^{-1} r_{\beta n}^{-1} \sin Q_n \\ i\mu_n r_{\beta n} \sin Q_n & \cos Q_n \end{pmatrix} = \begin{pmatrix} A_{11} & A_{12} \\ A_{21} & A_{22} \end{pmatrix} \tag{7}$$

, where $Q = kdr_\beta$. Here $k = p$(radiation frequency)$/c$, and d is the thickness of the n^{th} layer. From Equation (7), the relation of wave amplitudes of incident, reflected, and on the surface are derived as

$$S_n^{\searrow} / S_n^{\nearrow} = \frac{\mu_n r_{\beta n} A_{11} - A_{21}}{\mu_n r_{\beta n} A_{11} + A_{21}} \tag{8}$$

$$S_0 / S_n^{\nearrow} = \frac{2\mu_n r_{\beta n}}{\mu_n r_{\beta n} A_{11} + A_{21}} \tag{9}$$

It should be noted that Equation (8) is formed by a couple of conjugate complexities (numerator and denominator); therefore, the incident and reflected waves have equal absolute values of amplitudes, but different phases. This is as required by the energy conservation law.

In addition, we considered the attenuation of seismic wave amplitude. Guillier et al. (2005) also indicated the influence of attenuation (sometimes called the quality factor, Q value) was very important in smoothing bumps in HVSR from single-station ambient noise recordings. Because Q is inversely related to the strength of the attenuation, lower Q areas are more attenuating than higher Q areas (Shearer, 1999), and then an approximation, which is more suited for application in seismology, was derived (Aki and Richards, 1980; Shearer, 1999, Equation 6.83):

$$A(x) = A_0 e^{-\omega x / 2cQ} \tag{10}$$

where A_0 is the initial seismic wave amplitude, $A(x)$ is that after traveling along a distance x, and c and Q are related wave velocity and quality factor (i.e. when $c = Vp$, Q is the attenuation for P-waves (Qp); when $c = Vs$, Q is the attenuation for S-waves (Qs)).

Genetic Algorithm in the Joint Inversion

Genetic Algorithm (GA) is a powerful forward search technique used in computing a global optimum solution, but not a traditional inversion method. This technique was based on Darwin's evolutionism and invented by Holland (1975), and then developed by himself and his students. Different organisms (models) consist of different chromosomes (characteristics), which are strings of DNA. Parents reproduce offspring, after natural selection the superior ones can live and others were eliminated. By the biological process, the superior gene reserve and the offspring inherit more superior gene have higher probability to pass natural selection, subsequently they reproduce again. Finally, the most excellent organisms are born. GA use techniques inspired by biological process such as inheritance, crossover, selection, and mutation.

Two different fitness functions were used in this study. For the dispersion curve of phase velocities, a root mean square error (RMSE) type of fitness function was adopted.

$$RMSE = \sqrt{\frac{1}{n} \sum_{i=1}^{n} (C_{obs}(i) - C_{sim}(i))^2} \tag{11}$$

, where n is the number of data point of phase velocities, $C_{obs}(i)$ and $C_{sim}(i)$ mean the i^{th} data of the observed and simulated phase velocities, and then the fitness function of a dispersion curve was set as

$$Fitness_{DC} = \left(\frac{1}{1 + RMSE}\right)^{10} \tag{12}$$

Subsequently, the linear correlation was used for developing the fitness function of HVSR. Lin et al. (2008) used the linear correlation as the fitness function for the fitting between 1D transfer function of SH waves and HVSR of microtremor. Equation (12) is the linear correlation coefficient:

$$r = \frac{\sum_i (x_i - \overline{x})(y_i - \overline{y})}{[\sum_i (x_i - \overline{x})^2 \sum_i (y_i - \overline{y})^2]^{1/2}} \tag{13}$$

, where r is the linear correlation coefficient, $\overline{x}$ and $\overline{y}$ are the means of the xi and yi, respectively. It also termed product-moment correlation coefficient or Pearson's r (Press et al., 1992) to design a new fitness function because HVSR of microtremor and transfer function of SH waves are different in amplification on dominate frequency and on high frequency peaks and troughs. However, the fluctuations are similar on the frequency band near a dominate peak. The new fitness function of HVSR was set as:

$$Fitness_{HVSR} = (1 + r)/2 \tag{14}$$

The dispersion curve and HVSR inversions were integrated by the GA. The notable difference must be emphasized that the joint inversion in this study utilized the transfer function of SH waves to fit the HVSR of microtremor rather than the ellipticity of Raleigh wave that most studies used.

RESULTS AND DISCUSSIONS

Distribution of Vs30

The Vs30 values of 68 free-field TSMIP stations could be found via the website (http://egdt.ncree.org.tw/) of EGDT. The Vs30 of several of those stations with S-wave velocity profile less than 30 m were estimated by Kuo et al. (2011b) using the BCV extrapolation. The S-wave velocities were measured at six stations of the Taipei downhole arrays before the instruments were installed. So that we got the accurate Vs30 at 74 sites in this study, and those were used to sketch the distribution of Vs30 in the Taipei Basin (Fig. 3). Different colors represented various velocity intervals of S-wave as shown in the color bar. We set the velocity intervals referring to the Vs30 criteria of the NEHRP. The Vs30 at other points without velocities were interpolated using the Generic Mapping Tools (GMT). Otherwise, the logged stations were filled with different colors according to the site classification. Those filled with indigo are class B, filled with blue are class C, filled with green are class D, and filled with magenta are class E. The triangles represent the logged free-field TSMIP stations and the circles symbolize the logged stations of Taipei downhole arrays. Fig. 3 indicated most stations in the Taipei Basin being designated class D. Only several of those located near the edge of the basin have higher velocities and classified as class C; otherwise, sites of class E seems scattered randomly. On the other hand, the stations out of the basin obviously have higher velocities and most were classified as class C and B. In terms of the interpolated result of Vs30, the values are lower in the center of the basin and higher around the edge; however, no obviously pattern in common is apparent between the Vs30 and the Sungshan formation bottom contours.

Estimation of the S-wave Velocity Structures

The microtremor array surveys had been conducted at 12 strong motion station sites in the Taipei Basin. The 12 arrays were named after the TSMIP stations, they are, TAP003, TAP004, TAP007, TAP010, TAP014, TAP019, TAP022, TAP032, TAP037, TAP051, TAP089, and TAP091. Those arrays were conducted in different years that the strategies of measured durations are different as shown in Table 1. Different radii indicated that the layout of arrays depended on the space of each sites. However, the sampling rate was fixed as 100 points per second in all measurements.

First step of the data processing was to convert the data format to Seismic Analysis Code (SAC), and then check and correct the recordings using the functions of the SAC2000 software. After that, the high resolution F-K method was adopted to calculate phase velocities on several frequencies. The high resolution F-K technique is able to process the recordings of an artificial shaped array, which is conveniently to be arranged in a high populated downtown. The vertical component of velocity was extracted from the observed recordings and five different lengths of the moving window, i.e. 512, 1024, 2048, 4096, and 8192 points, were employed to calculate the spectra as shown in Fig. 4. Phase velocities were calculated from the resultant wavenumber of the maximum energy of F-K spectra. The observed phase velocities on the required frequencies at the 12 sites in the Taipei Basin were shown in Fig. 5. The phase velocities were similar on high frequencies but exhibited noteworthy differences on lower frequencies. The red and grey curves

indicated the limits for large and small arrays. In order to implement the joint inversion of phase velocities and HVSR, we calculated HVSR of microtremor at sites. The Fourier spectra of two horizontal and a vertical noise recordings were calculated, during the procedure, 6% cosine taper was used for each window of 4096 points. The HVSR were obtained by dividing the averaged horizontal spectrum by the vertical, and then smoothed 10 times. It is believed a conventional approach to assess site responses; nevertheless, it is able to be used to estimate S-wave velocity profiles in this study. The HVSR were shown in Fig. 6. The dominant frequencies and fluctuations of those HVSR were notable variable from site to site. This implies the variations of the sedimentary depths at those sites.

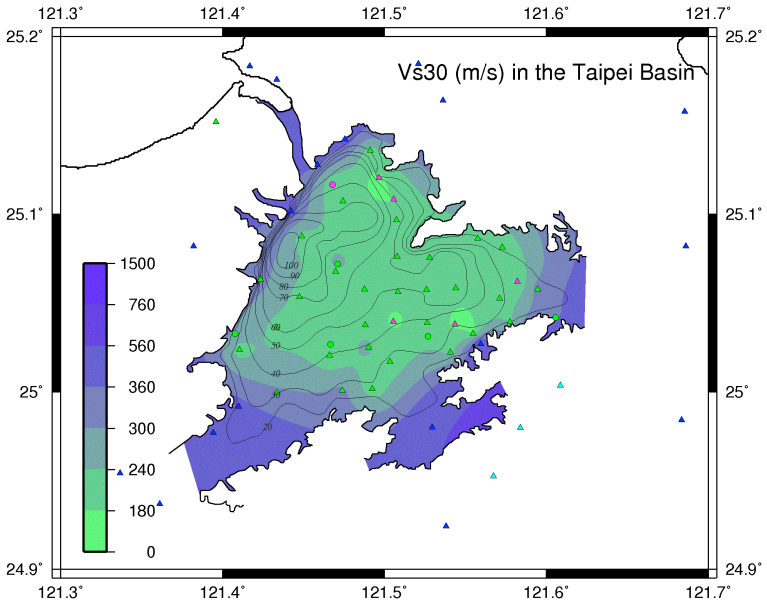

Fig. 3. The Vs30 values in the Taipei Basin were indicated by different colors. The contours (black curve) were the depth distributions of the Sungshan Formation bottom (Wang et al., 2004). The triangles are the logged free-field TSMIP stations; the circles are the logged stations of Taipei downhole arrays. The indigo color means the Vs30 is between 760 and 1500 m/s at the station; the blue color means the Vs30 is between 360 and 760 m/s at the station; the green color means the Vs30 is between 180 and 360 m/s at the station; the magenta color means the Vs30 is less than 180 m/s.

Table 1. Radii of the twelve microtremor arrays in the Taipei Basin. Two triple triangle arrays were conducted at TAP004, TAP007, TAP014, TAP032, TAP037, and TAP091; so that two measured durations of small and large arrays were listed.

Station	Rmin (m)	Rmax (m)	Measured Duration (min)
TAP003	8.0	32.0	110
TAP004	2.0	31.7	37+75
TAP007	3.0	56.0	75+75
TAP010	7.9	32.0	110
TAP014	2.0	32.0	37+75
TAP019	16.0	64.0	110
TAP022	16.0	64.0	110
TAP032	4.1	55.8	37+75
TAP037	3.8	64.3	37+75
TAP051	7.9	39.9	110
TAP089	7.9	32.1	110
TAP091	4.0	50.9	37+75

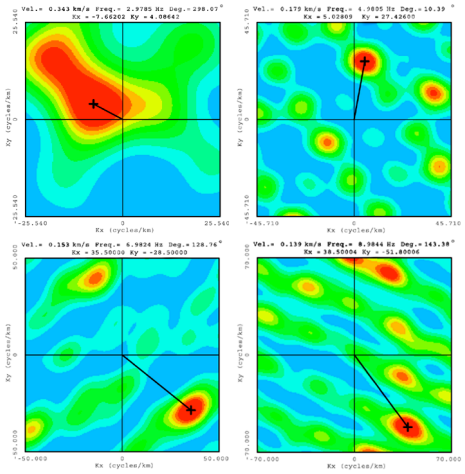

Fig. 4. The F-K spectra at TAP089 on 3, 5, 7, and 9 Hz. Vel is the phase velocity in km/s; Freq indicates the frequency in Hz; Deg gives the azimuth of the maximum propagating energy source clockwise from the north by degree; Kx and Ky mean the wavenumbers in the X and Y directions, respectively.

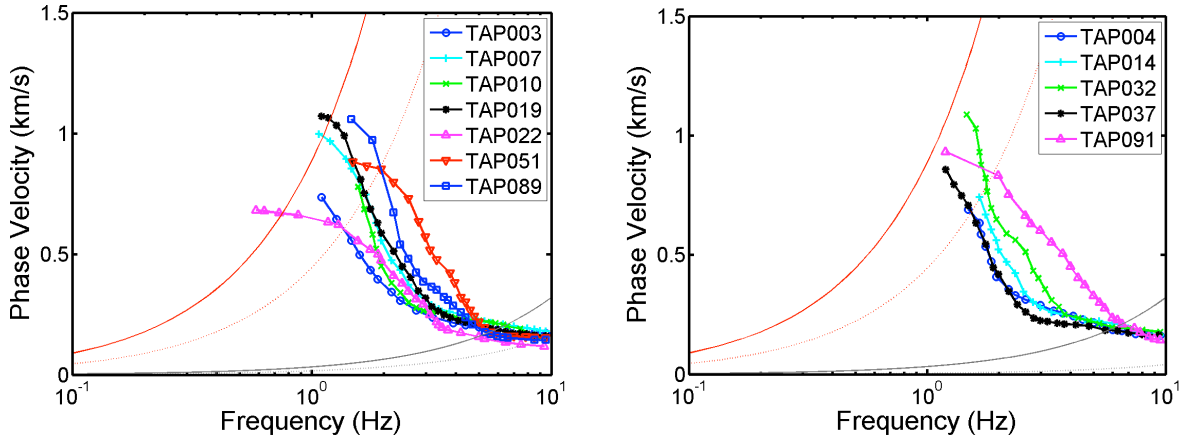

Fig. 5. The observed phase velocities at the 12 sites of the Taipei Basin.

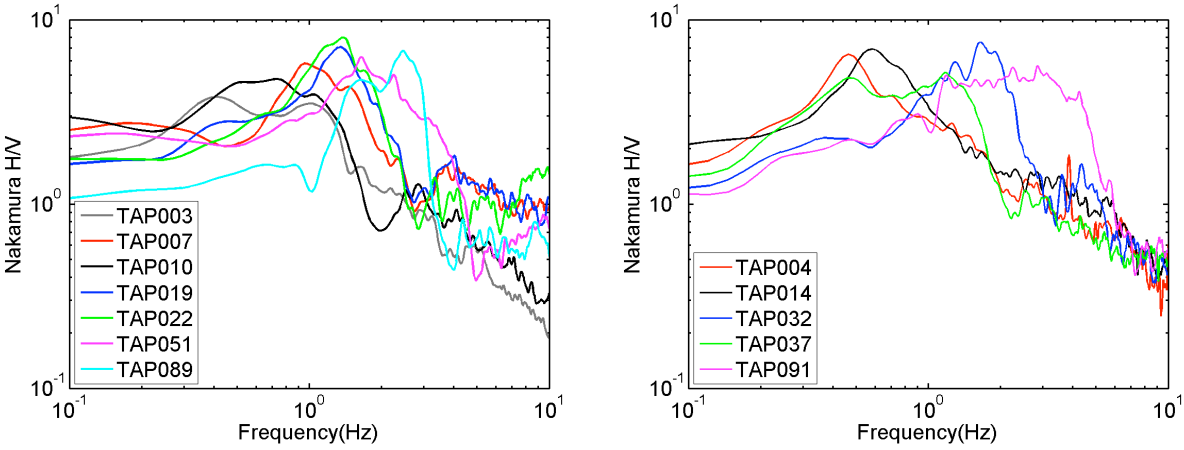

Fig. 6. The HVSR curves at the 12 sites of the Taipei Basin.

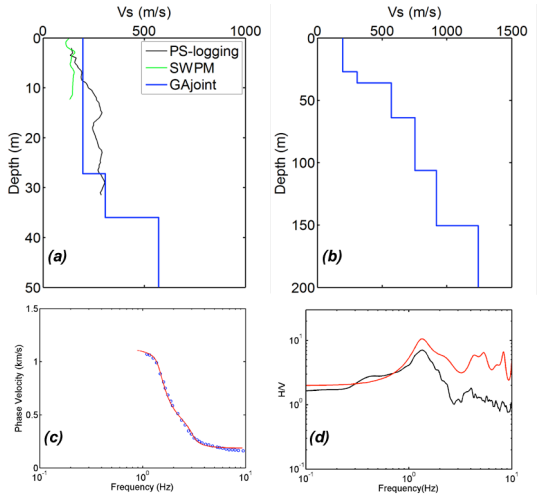

Fig. 7. The result of the joint inversion at TAP019. (a) The estimated S-wave velocity profile together with the profiles by PS-logging and SWPM. (b) The completed S-wave velocity structure. (c) The phase velocities (blue circle) and the best fitting dispersion curve (red line). (d) The HVSR (black) and best fitting simulated transfer-function of SH-wave (red).

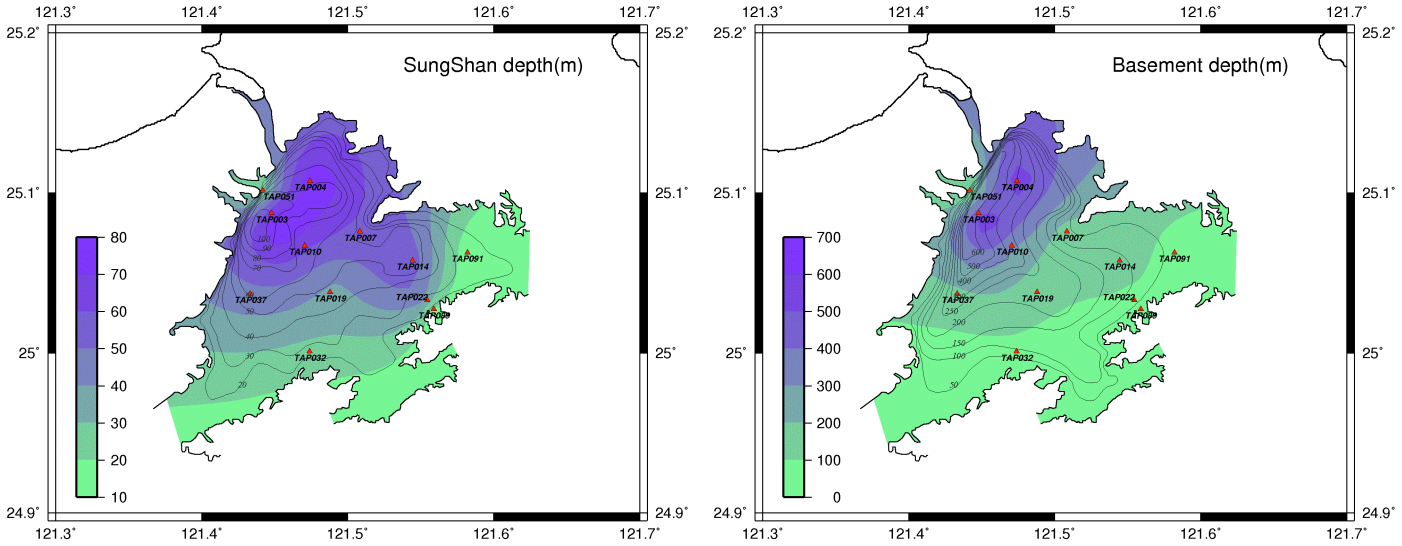

Fig. 8. Variations of the estimated depths of the Sungshan Formation bottom (left) and the basement top (right) in the Taipei Basin. Different colors indicated the results of this study; the black counters were the results of Wang et al. (2004) for comparison.

Consequently, the joint inversion method was implemented to estimate S-wave velocity structures at the 12 sites. Fig. 7 is a typical result at TAP019. Both the phase velocities and HVSR curve were well fitted by the simulated ones and thus it is convinced that the estimated S-wave velocity structure should be very close to the real subsurface structure. The shallow part of the estimated profile agreed with the result of PS-logging. Otherwise, the result indicated the depth to the Sungshan Formation (S-wave velocity smaller than 350 m/s) bottom and basement (S-wave velocity larger than 1000 m/s) top were about 40 and 150 m, respectively. We accomplished the joint inversions at the 12 sites to estimate the S-wave velocity profiles in the Taipei Basin, and the results were presented as in the Fig. 8. The estimated depths were illustrated with different colors as in the color bars. The results of Wang et al. (2004) were also plotted together for comparison. This figure focused the structures on the thicknesses of the upmost layer and the unconsolidated sediments. The upmost Sungshan Formation and the unconsolidated sediments were defined as with the S-wave velocity less than 350 and 1000 m/s in this study. The patterns of the results in Fig. 8 are roughly comparable to the black contours. However, according to our result the largest thicknesses of sedimentary layers are likely to appear in the north and northwest of the Taipei Basin. However, array survey is a lack in south of the basin, so that the depth variations were roughed out.

CONCLUSIONS

The array measurements of microtremor in this study were conducted in schools, and thus the sizes were constricted. However, it is believed that the well-pronounced peaks of HVSR are governed by the thickness of the unconsolidated sediments. We were therefore decided to develop a joint inversion technique to increase the detectable depth and estimate the whole velocity profile from surface to the basement. Otherwise, the particularly significant Vs30 were estimated by the velocity logging and an accurate extrapolation at 74 sites of the Taipei region as well as the Vs30 distribution in the basin was estimated. Consequently, the Vs30 is almost smaller than 360 m/s except for those near the basin edge. The thicknesses of the Sungshan Formation and the all sedimentary layers are thinner around the east and south edges, whereas both of which are thicker around the west edge especially in the north and northwest. However, we still lack of array in south of the basin that the depth variations were just roughed out in Fig. 8. Otherwise, we have no site in the north showed obvious thinning trend of estimated depth. It is still not enough to illustrate the completed S-wave velocity structures covering on the Tertiary bedrock using the measured arrays. For the shallower part we are collecting the results of logging; for the deeper part we are planning to conduct two or three more arrays to cover the south part of the basin, and then we will used the measured microtremor recordings of single stations to estimate more complete S-wave velocity structure of the Taipei Basin.

ACKNOWLEDGMENTS

We thank Dr. Wen-Gee Huang and Mr. Chi-Hsuan Chen for providing the logging data of Taipei downhole arrays. This research was funded by the National Science Council (NSC), Taiwan, under the grant No. NSC99-2116-M-492-005.

REFERENCES

Aki, K. [1957], "Space and time spectra of stationary stochastic waves, with special reference to microtremors", Bulletin of Earthquake Research Institute of Tokyo University, Vol. 35, No. 3, pp. 415-456.

Aki, K. and P. G. Richards [1980]. "*Quantitative Seismology: Theory and Methods*", W. H. Freeman and Company, 1st ed., 932 pp.

Anderson, J. G., Y. Lee, Y. Zeng, and S. Day [1996], "Control of strong motion by the upper 30 meters", Bull. Seism. Soc. Am., Vol. 86, No. 6, pp. 1749-1759.

Arai, H. and K. Tokimatsu [2004], "S-wave velocity profiling by inversion of microtremor H/V spectrum", Bull. Seism. Soc. Am., Vol. 94, No. 1, pp. 53-63.

Arai, H. and K. Tokimatsu [2005], "S-wave velocity profiling by joint inversion of microtremor dispersion curve and horizontal-to-vertical (H/V) spectrum", Bull. Seism. Soc. Am., Vol. 95, No. 5, pp. 1766-1778.

Arai, H. and K. Tokimatsu [2008], "Three-dimensional Vs profiling using microtremors in Kushiro, Japan", Earthq. Eng. Struct. Dyn., Vol. 37, pp. 845-859.

Bang, E. S. and D. S. Kim [2007], "Evaluation shear wave velocity profile using SPT based uphole method", Soil Dyn. Earthq. Eng., Vol. 27, No. 8, pp. 741-758.

Bodin, P. and S. Horton [1999], "Broadband microtremor observation of basin resonance in the Mississippi embayment, Central US", Geophys. Res. Lett., Vol. 26, No. 7, pp. 903-906.

Bonilla, L. F., J. H. Steidl, G. T. Lindley, A. G. Tumarkin, and R. J. Archuleta [1997], "Site Amplification in the San Fernando Valley, California: variability of site-effect estimation using the S-Wave, coda, and H/V methods", Bull. Seism. Soc. Am., Vol. 87, No. 3, pp. 710-730.

Boore, D. M. and M. W. Asten [2008], "Comparisons of shear-wave slowness in the Santa Clara Valley, California, using blind interpretations of data from invasive and noninvasive methods", Bull. Seism. Soc. Am., Vol. 98, No. 4, pp. 1983-2003.

Building Seismic Safety Council (BSSC) [2001], "*NEHRP recommended provisions for seismic regulations for new buildings and other structures, 2000 Edition. Part 1: Provisions*", prepared by the Building Seismic Safety Council for the Federal Emergency Management Agency (Report FEMA 368) Washington, D.C.

Capon, J. [1969], "High-resolution frequency-wavenumber spectrum analysis", *Proceedings of the IEEE*, Vol. 57, No. 8, pp. 1408-1418.

Fäh, D., F. Kind, and D. Giardini [2001], "A theoretical investigation of average H/V ratios", Geophys. J. Int., Vol. 145, pp. 535-549.

Fäh, D., F. Kind, and D. Giardini [2003], "Inversion of local S-wave velocity structures from average H/V ratios, and their use for the estimation of site-effects", J. Seismol., Vol. 7, pp. 449-467.

Fäh, D., G. Stamm, and H. B. Havenith [2008], "Analysis of three-component ambient vibration array measurements", Geophys. J. Int., Vol. 172, pp. 199-213.

García-Jerez, A., M. Navarro, F. J. Alcala, F. Luzon, J. A. Perez-Ruiz, T. Enomoto, F. Vidal, and E. Ocana [2007], "Shallow velocity structure using joint inversion of array and h/v spectral ratio of ambient noise: The case of Mula town (SE of Spain)", Soil Dyn. Earthq. Eng., Vol. 27, pp. 907-919.

Guillier, B., J. L. Chatelain, M. Hellel, D. Machane, N. Mezouer, R. Ben Salem, and E. H. Oubaiche [2005], "Smooth bumps in H/V curves over a broad area from single-station ambient noise recordings are meaningful and reveal the importance of Q in array processing: The Boumerdes (Algeria) case", Geophys. Res. Lett., Vol. 32, L24306.

Haskell, N. A. [1953], "The Dispersion of surface waves on multilayered media", Bull. Seism. Soc. Am., Vol. 43, No. 1, pp. 17-34.

Haskell, N. A. [1960], "Crustal reflection of plane SH waves", J. Geophys. Res., Vol. 65, pp. 4147-4150.

Holland, J. H. [1975]. "*Adaptation in Natural and Artificial Systems: An Introductory Analysis with Applications to Biology, Control, and Artificial Intelligence*", University of Michigan Press, 183 pp.

Horike, M. [1985], "Inversion of phase velocity of long-period microtremors to the S-wave-velocity structure down to the basement in urbanized areas", Journal of Physics of the Earth, Vol. 33, pp. 59–96.

Kawase, H., T. Satoh, T. Iwata, and K. Irikura [1998], "S-wave velocity structure in the San Fernando and Santa Monica areas", *Proceedings of the 2nd International Symposium on the Effects of Surface Geology on Seismic Motion*, Vol. 2, pp. 733–740.

Kuo, C. H., D. S. Cheng, H. H. Hsieh, T. M. Chang, H. J. Chiang, C. M. Lin, and K. L. Wen [2009], "Comparison of three different methods in investigating shallow shear-wave velocity structures in Ilan, Taiwan", Soil Dyn. Earthq. Eng., Vol. 29, No. 1, pp. 133-143.

Kuo, C. H., K. L. Wen, H. H. Hsieh, T. M. Chang, C. M. Lin, and C. T. Chen [2011a], "Evaluating empirical regression equations for Vs and estimating Vs30 in northeastern Taiwan", Soil Dyn. Earthq. Eng., Vol. 31, No. 3, pp. 431-439.

Kuo, C. H., K. L. Wen, H. H. Hsieh, C. M. Lin, and T. M. Chang [2011b], "Site classification of free-field TSMIP stations using the logging data of EGDT". (Submitted)

Lermo, J. and F. J. Chavez-Garcia [1993], "Site effect evaluation using spectral ratios with only one station", Bull. Seism. Soc. Am., Vol. 83, No. 5, pp. 1574–1594.

Lin, C. M., K. L. Wen, C. H. Kuo, H. J. Chiang, and L. T. Son [2008], "Site characteristic analyses of microtremor in Hanoi region, Vietnam", *Proceeding of the 2008 Taiwan-Japan Symposium on the Advancement of Urban Earthquake Hazard Mitigation Technology*, 53-56, Taoyuan, Taiwan.

Louie J. N. [2001], "Faster, better: shear-wave velocity to 100 meters depth from refraction microtremor arrays", Bull. Seism. Soc. Am., Vol. 91, No. 2, pp. 347-364.

Malagnini, L., A. Rovelli, S. E. Hough, and L. Seeber [1993], "Site amplification estimates in the Garigliano valley, central Italy, based on dense array measurements of ambient noise", Bull. Seism. Soc. Am., Vol. 83, No. 6, pp. 1744–1755.

Matsushima, T. and H. Okada [1990], "Determination of deep geological structures under urban areas using long-period microtremors", Butsuri Tansa, Vol. 43, pp. 21–33.

Nakamura, Y. [1989], "A method for dynamic characteristics estimation of subsurface using microtremor on the ground surface",

Quarterly Report of RTRI, Vol. 30, No. 1, pp. 25-33.

Nakamura, Y. [2007], "Characteristics of H/V spectrum", *NATO Advanced Research Workshop*, Dubrovnik, Croatia.

Pancha, A., J. G. Anderson, J. N. Louie, and S. K. Pullammanappallil [2008], "Measurement of shallow shear wave velocities at a rock site using the ReMi technique", Soil Dyn. Earthq. Eng., Vol. 28, pp. 522-535.

Parolai, S., M. Picozzi, S. M. Richwalski, and C. Milkereit [2005], "Joint inversion of phase velocity dispersion and H//V ratio curves from seismic noise recordings using a genetic algorithm, considering higher modes", Geophys. Res. Lett., Vol. 32, No. 1, L01303.

Press, W. H., S. A. Teukolsky, W. T. Vetterling, and B. P. Flannery [1992], "*Numerical Recipes in Fortran 77: The Art of Scientific Computing*", Cambridge University Press, vol. 1, 2nd ed., 1008 pp.

Sato, T., H. Kawase, M. Matsui, and S. Kataoka [1991], "Array measurement of high frequency microtremors for underground structure estimation", *Proceedings of 4th International Conference on Seismic Zonation*, 2, pp. 409–416.

Satoh, T., H. Kawase, T. Iwata, S. Higashi, T. Sato, K. Irikura, and H. C. Huang [2001a], "S-wave velocity structure of the Taichung Basin, Taiwan, estimated from array and single-station records of microtremors", Bull. Seism. Soc. Am., Vol. 91, No. 5, pp. 1267-1282.

Satoh, T., H. Kawase, and S. Matsushima [2001b], "Estimation of S-wave velocity structures in and around the Sendai Basin, Japan, using array records of microtremors", Bull. Seism. Soc. Am., Vol. 91, No. 2, pp. 206-218.

Shearer, P. M. [1999], "*Introduction to Seismology*", Cambridge University Press, 1st ed., 260 pp.

Tsuboi, S., M. Saito, and Y. Ishihara [2001], "Verification of horizontal-to-vertical spectral-ratio technique for estimation of site response using borehole seismographs", Bull. Seism. Soc. Am., Vol. 91, No. 3, pp. 499-501.

Wang, C. Y., Y. H. Lee, M. L. Ger, and Y. L. Chen [2004], "Investigating subsurface structures and P- and S-wave velocities in the Taipei Basin", Terr. Atmos. Ocean. Sci., Vol. 15, No. 4, pp. 609-627.

Wen, K. L., T. M. Chang, C. M. Lin, and H. J. Chiang [2006], "Identification of nonlinear site response using the H/V spectral ratio method", Terr. Atmos. Ocean. Sci., Vol. 17, No. 3, pp. 533-546.

Williams, R. A., J. K. Odum, W. J. Stephenson, and R. B. Herrmann [2007], "Shallow P- and S-wave velocities and site resonances in the St. Louis region, Missouri-Illinois", Earthq. Spectra, Vol. 23, No. 3, pp. 711–726.

Woolery, E. W. and R. Street [2002], "3D near-surface soil response from H/V ambient-noise ratios", Soil Dyn. Earthq. Eng., Vol. 22, pp. 865-876.